



ARTICLE

Analysis of a Water-Cooled Unit under Different Loads

Daoming Shen^{1,*}, Jinhong Xia¹, Chao Gui¹ and Songtao Xue²

¹Xinxiang University, Xinxiang, 453000, China

²Department of Architecture, Tohoku Institute of Technology, Sendai, 982-8577, Japan

*Corresponding Author: Daoming Shen. Email: shendaoming@163.com

Received: 14 June 2022 Accepted: 13 September 2022

ABSTRACT

In order to ensure the safe operation of the compressors used in water chillers, in the present study some interlock protections have been added to the related design. These include a low pressure protection, a high pressure protection, an exhaust temperature protection and a differential pressure protection. Some tests have been conducted by tuning the saturation suction and exhaust temperatures of the compressor through adjustment of the cold source outlet temperature and the ambient temperature. The results show that the ambient temperature increases with decreasing device load and increasing fan speed under the same saturated suction temperature; the device refrigerating capacity steps up with augmenting load and dropping saturation exhaust temperature, while it is not greatly affected by the fan speed. Moreover, the Energy efficiency ratio (COP) decreases with the rise of the saturation exhaust temperature. This parameter is not affected much by the device load and fan speed at high saturation exhaust temperature, while it improves on increasing the device load and decreasing the fan speed at low saturation exhaust temperature.

KEYWORDS

Ambient temperature; cold source temperature; refrigerating capacity; Energy efficiency ratio (COP); fan speed; load

Nomenclature

C_p	the specific heat capacity of a refrigerant at constant pressure, kJ/(kg·°C)
G_r	the circulating flow of working medium, kg/s
G_w	the circulating flow of refrigerant, kg/s
h_{in}/h_{out}	the enthalpy value at the inlet and outlet of working medium in an evaporator, kJ/kg
P_{com}	the consumption power of a compressor, kW
P_{fan}	the consumption power of fan, kW
P_{pump}	the consumption power of water pump, kW
P_{total}	energy consumption of the device, kW
Q	refrigerating capacity of the unit, kW
Q_r	the heat absorption of working medium in the evaporator, kW
Q_w	cooling capacity of refrigerant in the evaporator, kW
T_{in}/T_{out}	the inlet and outlet temperature of the refrigerant, °C
COP	the index to evaluate the comprehensive performance of the device, Dimensionless quantity
η	heat balance error of evaporator, Dimensionless quantity



1 Introduction

With the advantages of large load change and long refrigeration cycle, large scale water-cooled units are mainly used in subway, high-rise buildings, apartments, engineering, and other places. As the main energy consumption products, many scholars [1–5] have studied a series of problems such as equipment control logic, equipment selection, device performance, fault analysis, structural lubrication, application environment, etc. Refrigeration and air-conditioning compressors are designed to work under well-defined conditions. In some applications, it is interesting to observe their performances beyond these conditions [6–8], for example, in the case of an air source under different loads.

Through experiments, Cuevas et al. [1,2] measured the performance of the scroll refrigeration compressor under the condition of variable speed and multiple pressure ratios. It was pointed out that the compressor used achieved the highest volume efficiency and isentropic efficiency when the pressure ratio was between 2.2 and 2.6. With the increase in pressure ratio, the internal leakage increased, the lubrication condition became worse, and the volume efficiency and isentropic efficiency decreased.

Ibrahim et al. [3] simulated the condenser coil of the air source heat pump water heater, studied the influence of the length of the condenser coil on the performance of the heat pump, and finally determined the shortest length of the condenser coil matching the best energy efficiency considering the cost factor, simulated the condenser coil of the air source heat pump water heater, studied the influence of the length of the condenser coil on the performance of the heat pump, and finally determined the shortest length of the condenser coil matching the best energy efficiency considering the cost factor.

Fan et al. [6] verified the application of unbalanced data technology in the fault diagnosis of water chillers. Firstly, the fault samples were oversampled by using the synthetic minority oversampling technology (smote), and then the fault diagnosis was carried out by using the support vector machine (SVM). Liu et al. [7] took the group of chillers with the non-uniform matching of cooling capacity as the research object, considered the selfbalance characteristic of cooling capacity, constructed the thermal characteristic model of parallel operation of multiple chillers, studied the parallel operation characteristic of non-uniform load matching chillers under variable load, and proposed the control strategy of multiple Chillers Based on energy efficiency benchmark, Compared with the uniform load matching chiller, the applicability of the non-uniform load matching control strategy is discussed. Tang et al. [8] established the theoretical model of the air-cooled refrigeration system based on the polyphase lumped parameter method, mass conservation, energy conservation, and pressure balance, and carried out theoretical research and experimental analysis on the air-cooled refrigeration system. Based on the non-linear temperature enthalpy relationship of mixed refrigerants during heat exchange, the influence of mixed refrigerants bubble, dew point temperature, and slip temperature on cooling capacity was analyzed. Yu et al. [9] conducted experimental research on the performance of different mixed refrigerants. Li [10] summarized the oil return effect of an air pump, thermosiphon, and ejector in screw chiller.

Kamil investigated the steam condensation phenomena in an air-cooled condenser [11]. The considered horizontal flattened tube has a 30 mm hydraulic diameter, and its length is a function of the steam quality with a limit value between 0.95 and 0.05. Mahmood et al. used the Engineering Equation Solver (EES) to solve a set of methodical equations and empirical equations, the mathematical model of the current study, which has been validated with experimental results from the literature [12,13].

In addition, it is very important to study the effect of application environment on the performance of the chiller. Mao et al. [14] compared the thermophysical properties of R22 and R147a under different mixing ratios with the indexes of compressor suction and exhaust pressure, suction and exhaust temperature, power, unit heating capacity, and energy efficiency ratio. It was confirmed by experiments that the unit heating capacity and COP of R22 and R147a mixed refrigerant system with the ratio of 7:3 were slightly lower than those of the R22 system, while the suction and exhaust pressure, suction and exhaust

temperature, and compressor power were all lower than those of R22 system. Experimental research on the influence of the performance of different heat pump units and factors, for example, environmental temperature, water supply temperature, air volume, water supply flow, and other variables on cop, heating capacity, system power consumption, energy efficiency, exhaust temperature, compression ratio and so on, also were carried out in china and other countries [15–26].

Kasim et al. aimed to reduce the required cooling capacity of an absorption chiller powered by a solar parabolic trough collector and a backup fuel boiler by integrating thermal storage tanks [27]. The system's thermal performance was simulated for a building that is cooled for 14 h/day. The system used 1000 m² parabolic trough collector with 1020 kW absorption chiller. Chilled water storage and cooling water storage effects on the system performance for different operation hours per day of the absorption chiller under Izmir (Turkey) and Phoenix (USA) weather conditions were analyzed.

As the compressor performance is very important to the operation of the whole equipment, and the saturation temperature of the compressor suction and exhaust will have a direct impact on the performance of the compressor, therefore, referring to the former research results and based on the existing equipment, this paper describes the reasonable operation conditions of the compressor. It takes the satisfaction of the compressor suction and exhaust temperature as the benchmark, carries out the environmental temperature and the refrigerant outlet temperature adjustment, and then analyzes the influence of load and air volume on the performance of the air source chiller under different loads, so as to provide direction for further improvement of the performance of the device. By selecting appropriate refrigerants and equipment, determining reasonable index parameters, and to improve the energy consumption ratio, so as to be better applied and popularized in practical projects.

2 Chiller Prototype and Experimental Device

The system principle of the water chiller is shown in Fig. 1. The equipment is mainly composed of a parallel compressor unit, oil separator, microchannel heat exchanger, mass flowmeter, electronic expansion valve, spray expansion valve, gas-liquid separator, hot gas expansion valve and other main components.

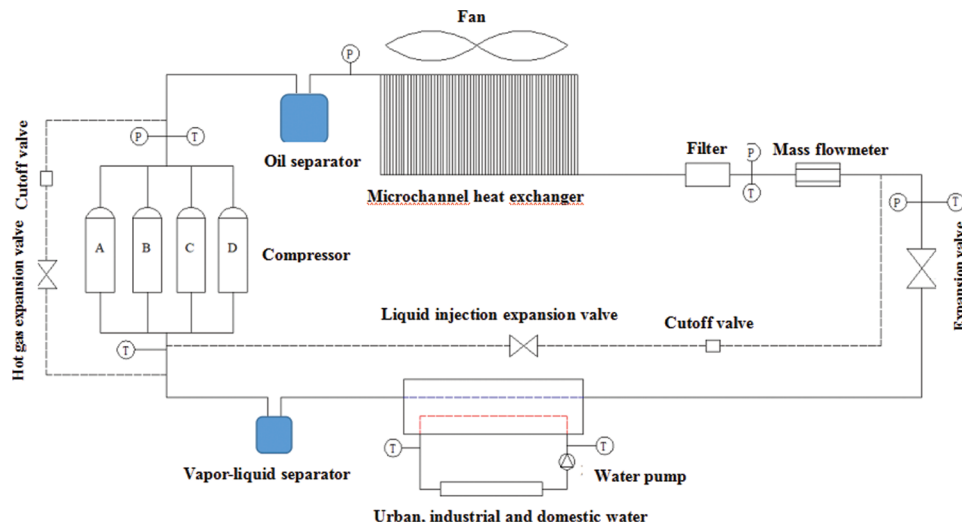


Figure 1: Schematic diagram of equipment system

The parallel compressor unit is composed of four SZ148 Danfoss constant frequency scroll compressors. During the operation of the equipment, the load of the unit is mainly controlled by adjusting the number of

compressors. In order to ensure that the compressor operates within the normal temperature/pressure working condition range, and avoid the compressor's protection shutdown caused by differential pressure protection, exhaust protection, high-pressure protection, etc., the experiment respectively sets the liquid injection expansion valve and hot gas expansion valve to control the suction state of the compressor. Among them, the type of spray expansion valve is Sporlan. When the wall temperature of the compressor is high, the opening of the spray valve is automatically controlled so as to effectively cool down the compressor; The thermal gas expansion valve adopts Danfoss TGEX-11TR expansion valve, whose function is similar to a bypass device. After throttling, the exhaust gas of the compressor is fully mixed with the compressor evaporator exhaust gas at the suction port of the compressor so as to prevent the compressor suction from carrying liquid.

In order to reduce the occupied volume of equipment space, the microchannel with high heat exchange efficiency is selected as the condenser, and the air temperature at the inlet and outlet of the microchannel is measured by the enthalpy difference method. The thermocouple is installed in the temperature sampler, and the air temperature is measured by dry bulb temperature. A variable frequency fan is selected to provide power for airflow. During the experimental operation, the number of variable frequency fans remains unchanged. The air flow is controlled by adjusting the speed of the variable frequency fan (see Fig. 2 for specific installation). In addition, an MIK-P300 pressure transmitter is used to measure the working medium pressure, with the measurement accuracy of 0.1 level; WZP thermal resistance is employed to measure the working medium/cold source temperature in the device, with the measurement range of $-200^{\circ}\text{C}\sim 500^{\circ}\text{C}$, and the measurement accuracy of $\pm 0.15^{\circ}\text{C}$; The DMF-1-U20 mass flowmeter is selected to measure the working fluid flow. The measuring range is $0\sim 3000\text{ kg/h}$, and the measuring accuracy is $\pm 0.1\%$. The thermocouple probe is installed on the surface of the compressor housing with tin paper, and then the wall temperature of the compressor is measured.

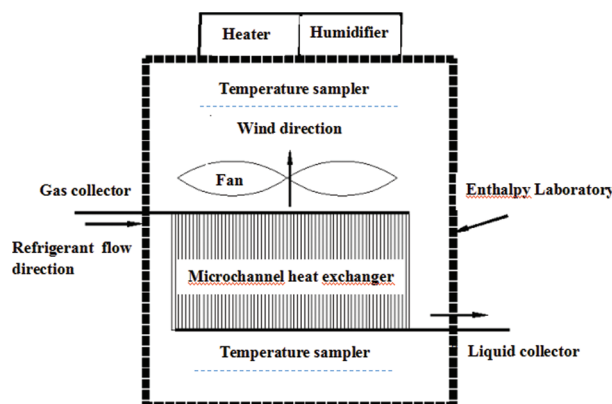


Figure 2: Measurement of air source condition

For a specific load, the experiment first determines the circulating flow of the refrigerant in the device under the condition that the inlet and outlet temperature of the refrigerant is $12^{\circ}\text{C}/7^{\circ}\text{C}$ and the dry and wet bulb temperature of the air source is $35^{\circ}\text{C}/34^{\circ}\text{C}$, and then adjusts the outlet temperature of the refrigerant and the dry bulb temperature of the air source to reach the set value of the saturated suction and exhaust temperature within the operating condition range of the compressor.

3 Calculation of Experimental Data

In the experiment, the supercooling of the expansion valve is 5°C , and the suction superheat of the compressor is 8°C . According to the temperature, pressure, flow, and other parameters measured by the

instrument, the heat absorption of the working medium in the evaporator can be obtained:

$$Q_r = G_r(h_{out} - h_{in}) \quad (1)$$

where: G_r is the circulating flow of the working medium, kg/s; h_{in}/h_{out} is the enthalpy value at the inlet and outlet of working medium in an evaporator, which can be calculated according to the temperature/pressure value at the inlet of the expansion valve and the suction port of compressor, kJ/kg.

Cooling capacity of refrigerant in evaporator:

$$Q_w = G_w C_p (T_{in} - T_{out}) \quad (2)$$

where: G_w is the circulating flow of refrigerant, kg/s; C_p is the specific heat capacity of the the refrigerant at constant pressure, kJ/(kg·°C); T_{in}/T_{out} is the inlet and outlet temperature of refrigerant, °C.

Experiment regulation: when the errors of the heat balance of evaporator are less than 3%, the experiment data are valid, and the arithmetic mean value of heat exchange of working medium and refrigerant were used as the calculation standard of refrigerating capacity of the device, namely:

Heat balance error of evaporator:

$$\eta = |Q_r - Q_w| / (Q_r + Q_w) \quad (3)$$

Refrigerating capacity of the unit:

$$Q = (Q_r + Q_w) / 2 \quad (4)$$

In the calculation of energy consumption of the device, the main elements include compressor, water pump, and fan. The input voltage can calculate the power consumption and current, that is:

$$P_{total} = P_{con} + P_{pump} + P_{fan} \quad (5)$$

where: P_{com} is the consumption power of a compressor, kW; P_{pump} is the consumption power of water pump, kW; P_{fan} is the consumption power of the fan, kW.

Finally, COP is selected to evaluate the comprehensive performance of the device, namely:

$$COP = Q / P_{total} \quad (6)$$

4 Analysis of Experimental Data

The protection of compressor suction and exhaust state mainly includes high-pressure protection, low-pressure protection, and exhaust temperature protection. Among them, low-pressure protection aims to avoid system energy efficiency reduction, liquid refrigerant freezing, and other faults caused by low suction pressure; Because of when the exhaust pressure is high, the exhaust temperature increases, the high-pressure protection is set, the compression ratio increases and the volumetric efficiency decreases, so that the cooling capacity decreases, the power consumption increases, and the compressor efficiency decreases; The exhaust temperature protection mainly limits the exhaust temperature of the compressor. If the exhaust temperature exceeds the normal value. In that case, it will not only lead to the carbonization corrosion of the lubricating oil, reduce the viscosity of the lubricating oil, thus reducing the lubricating performance, resulting in poor lubrication, accelerated wear, and increased power consumption, but also cause permanent damage to the compressor volute, drive bearing, internal seal, etc.

The working condition operation diagram of the scroll compressor used in the device is shown in Fig. 3. It can be seen from the diagram that the saturated suction temperature range of the compressor is $-30^{\circ}\text{C} \sim 25^{\circ}\text{C}$, and the saturated exhaust temperature range is $10^{\circ}\text{C} \sim 60^{\circ}\text{C}$. In order to ensure the safe and reliable operation of the compressor, the corresponding protection is also set for the compressor, in which, the first stage indicates

the low-pressure protection of the compressor, the second stage means the high-pressure protection of the compressor, and the third stage expresses the compressor exhaust temperature protection. In addition, in order to ensure the safe operation of the device, the compressor differential pressure protection is specially designed, as shown in Fig. 3 (the fourth stage); that is, the compressor must provide certain power for the working medium to overcome its flow resistance in the condenser, liquid pipeline, expansion valve, evaporator, and other components.

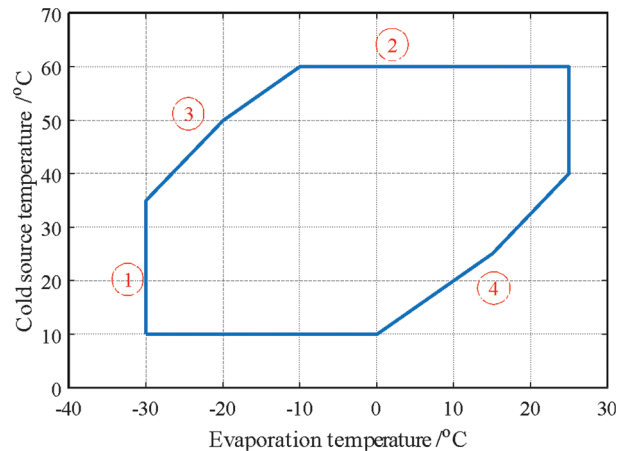


Figure 3: Operation map of compressor

During the experimental operation, other operating conditions remain unchanged. The saturated suction temperature and saturated exhaust temperature of the compressor are adapted respectively by adjusting the refrigerant's outlet temperature and ambient temperature. Among them, the saturated suction temperature and saturated exhaust temperature go up with the heightening of the outlet temperature and ambient temperature of the refrigerant, which is mainly caused by the temperature difference of heat exchange.

Furthermore, the full load working medium flow rate is more than 75%, and the full load working medium flow rate is more than 50%. Although the speeding up of the working medium flow rate in the heat exchanger results in the enhancement of the heat transfer characteristics and the downsizing of the heat exchange temperature difference, the condensation heat exchange is the largest under the full load condition, and the enhancement of the heat exchange makes the heat exchange temperature difference much higher. Finally, under the same saturated suction and exhaust temperature, the full load will affect the outlet temperature, and the ambient temperature of the refrigerant should be lower, as shown in Fig. 4.

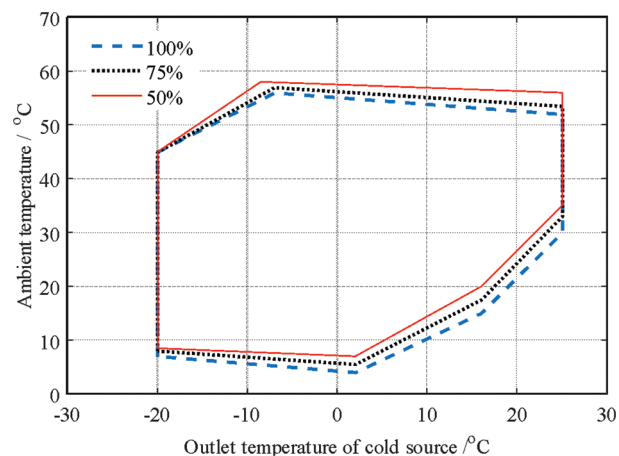


Figure 4: Environment range provided by refrigeration equipment under different load

Under the same working condition, the full load cooling capacity value is equal to $(1.32\sim 1.42) \times 75\%$ load cooling capacity, and load cooling capacity value is equal to $(1.88\sim 2.06) \times 50\%$ load cooling capacity, because the compressor is the main power for the flow of working fluid in the device. When the number of starting and stopping compressors are different, it will inevitably lead to different cycle flow of working fluid, and then the device will show different cooling effects. In addition, under the condition of the same refrigerant outlet temperature (i.e., under the condition of compressor saturated suction temperature), the refrigerating capacity improves with the reduction of ambient temperature, because: the decrease of ambient temperature results in the decrease of saturated compressor exhaust, while the volumetric compressor efficiency raises with the reduction of pressure ratio, resulting in the speeding up of working medium circulation flow, thus showing a greater refrigerating capacity [25,26], which is shown in Fig. 5.

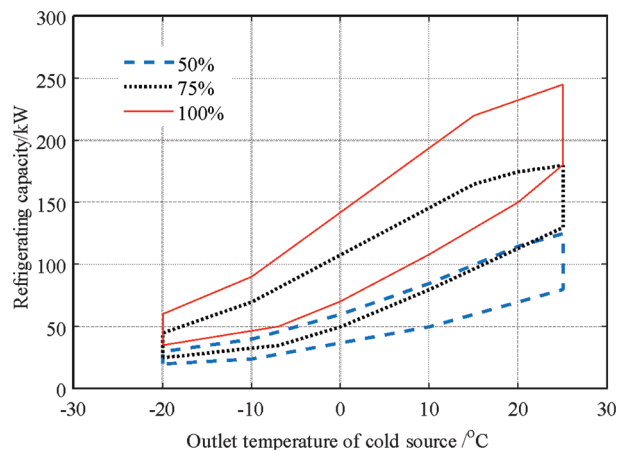


Figure 5: Refrigerating capacity providing by refrigeration equipment under different load

For the same type of parallel compressor unit, when evaluating the COP of the device, the comprehensive performance of a single compressor can be characterized. When the saturated exhaust gas of the compressor is large, the compression ratio also augments, while the compressor's isentropic efficiency decreases with the compressor decreases with the increase of pressure ratio [28,29]. Therefore, under the same saturated suction temperature condition of compressor, Power consumption will go up with the increase of pressure ratio, that is to say, under the same saturated suction condition, the power consumption of compressor increases with the rising of saturated exhaust temperature, while the refrigerating capacity improved with the saturated exhaust gas as the temperature becomes higher, the COP of the device becomes less; In addition, under the same compressor suction and exhaust saturation temperature condition, the difference between different load conditions increases with the falling of saturated exhaust temperature, and when the exhaust temperature takes the maximum value, the COP difference between different load conditions is very small, as shown in Fig. 6.

Under the condition that the following influencing factors remain unchanged, the influence of fan speed on equipment performance is studied and analyzed, such as cold source outlet temperature/flow, ambient temperature, superheat and subcooling. With the condition of 50% load, different fan speeds, and specific compressor saturated exhaust temperature, the ambient temperature goes up with the increase of fan speed. When the fan speed increases by 200 r/min, the ambient temperature ascends by about $0.218^{\circ}\text{C}\sim 2.828^{\circ}\text{C}$, and the difference grows with the falling of saturated exhaust temperature. This is because: under the same heat exchange and saturated exhaust temperature conditions, the air volume increases with the up-grading of fan speed, resulting in the diminution of heat exchange temperature difference, i.e., the going up of ambient temperature; and with the downsize of saturated exhaust

temperature, the condensation heat exchange gradually increases, resulting in the further becomes large to heat exchange temperature difference between various fan speeds, as shown in Fig. 7.

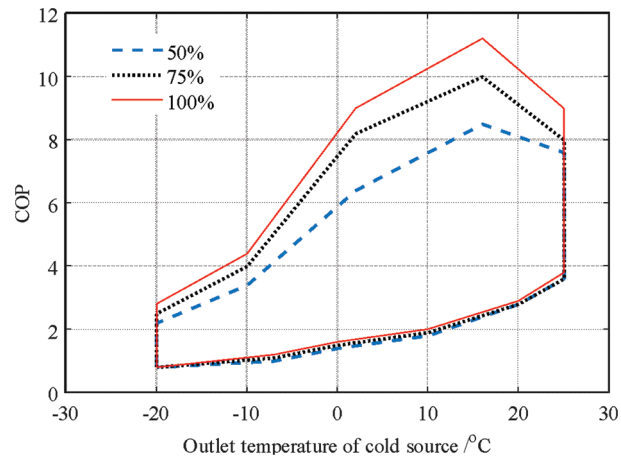


Figure 6: COP variation range of equipment performance under different load

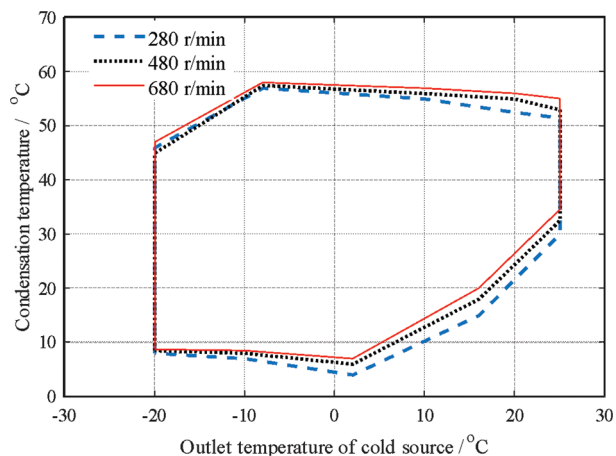


Figure 7: Environment range providing by refrigeration equipment under different fan speed

In addition to the influence of wind speed on the heat transfer characteristics of the condenser, it also has an indirect effect on the precooling in front of the valve. However, the supercooling change will not greatly impact the heat transfer of the evaporator. Therefore, the influence of wind speed on the refrigerating capacity of the unit is relatively small; that is, the change of refrigerating capacity with wind speed is relatively small; In addition, under the same wind speed and suction saturation temperature conditions, the refrigerating capacity attenuates with the raise of saturated exhaust temperature. Similarly, as mentioned above, the higher saturated exhaust temperature causes the magnification of compressor pressure ratio, thus making the compression volume efficiency lower, inducing the working medium circulation flow diminution, and finally reducing the overall refrigerating capacity of the device, as shown in Fig. 8.

The COP of the device changes with the experimental variables, which is a comprehensive reflection of the different effects of the experimental variables on the refrigerating capacity and the total power consumption of the device. Under the same condition, COP weakens with the going up of saturated exhaust temperature. Under the condition of high saturated exhaust temperature, wind speed has little

effect on COP, while under the condition of low saturated temperature, COP will boost with the decrease of wind speed, as shown in Fig. 9.

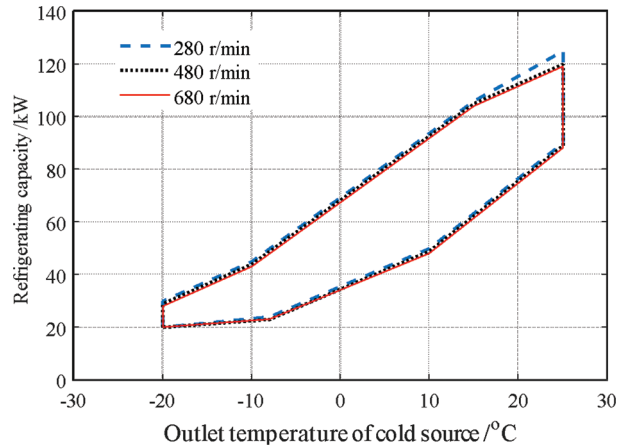


Figure 8: Refrigerating capacity providing by refrigeration equipment under different fan speed

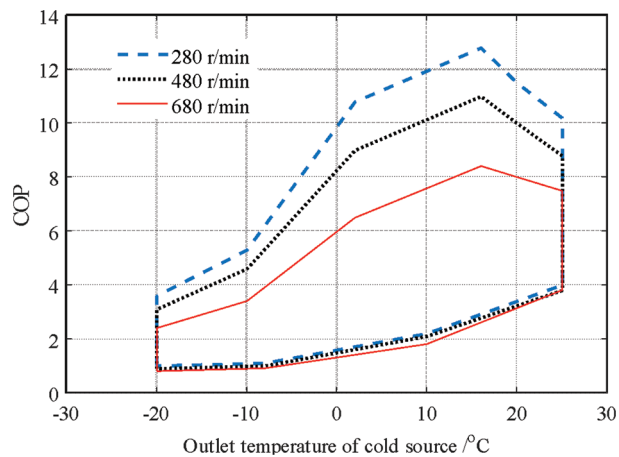


Figure 9: COP variation range of equipment performance under different fan speed

The former is due to the low isentropic efficiency of the compressor at high saturated exhaust temperature. At this time, the power consumption of the compressor accounts for a large proportion of the total power consumption of the device. Although the reduction of wind speed will cut down the total power consumption of the fan, it has little impact on the total power consumption of the device. The latter is due to the improvement of the isentropic efficiency of the compressor at low saturated exhaust temperature (that is, the power consumption of the compressor accounts for the total power consumption of the device). The wind speed has a great influence on the COP of the device, and the wind speed mainly improves the COP of the device by reducing the power consumption of the device, but has little influence on the cooling capacity.

5 Conclusion

In this paper, the air source water chiller is taken as the experimental research object. By adjusting the outlet temperature of the cold source and the ambient temperature, the compressor's saturated suction and

exhaust temperature of the compressor was adjusted. The influence of the system performance of the air source water chiller under different loads is studied; the conclusion and future directions are as follows:

1. In order to ensure the stable and reliable operation of the compressor, the operation protection of the compressor mainly includes compressor low-pressure protection, compressor high-pressure protection, compressor exhaust temperature protection and compressor differential pressure protection;
2. Through adjusting the outlet temperature and ambient temperature of the cold source, the saturated suction and exhaust temperature of the compressor is adjusted. Under the same saturated suction temperature, the ambient temperature increases with the decrease of the unit load and the increase of the wind speed;
3. The refrigeration capacity of the unit improves with the increase of the load and the dropping of the saturated exhaust temperature (the coming down of the ambient temperature), but it is not affected by the wind speed;
4. The purpose of COP analysis is to comprehensively evaluate the performance of the device. Under the same saturated suction temperature condition, the compressor power consumption increases with the increase of saturated exhaust temperature, and the cooling capacity declines with the increase of saturated exhaust temperature, resulting in cop decreasing with the increase of saturated exhaust temperature. In addition, under the high saturated exhaust temperature condition, COP is affected by the device load, wind speed, etc. The COP promotes the increase of load and the slower wind speed under the condition of low saturated exhaust temperature;
5. Further, the device should be optimized, select appropriate refrigerants and equipment, determine reasonable index parameters, and improve the energy consumption ratio, so as to be better applied and popularized in practical projects.

Funding Statement: This work was supported by the National Natural Science Foundation of China (No. 41877251) and Major Science and Technology Projects of Xinxiang City (No. 21ZD012).

Conflicts of Interest: The authors declare they have no conflicts of interest to report regarding the present study.

References

1. Cuevas, C., Lebrun, J., Lemort, V., Winandy, E. (2010). Characterization of a scroll compressor under extended operating conditions. *Applied Thermal Engineering*, 30(6–7), 605–615.
2. Cuevas, C., Lebrun, J. (2010). Testing and modelling of a variable speed scroll compressor. *Applied Thermal Engineering*, 30(2–3), 469–478.
3. Ibrahim, O., Fardoun, F., Younes, R., Hasna, L. (2014). Air source heat pump water heater: Dynamic modeling, optimal energy management and mini-tubes condensers. *Energy*, 64, 1102–1116.
4. Bendapudi, S., Braun, J. E., Groll, E. A. (2008). A comparison of moving-boundary and finite volume formulations for transients in centrifugal chillers. *International Journal of Refrigeration*, 31, 1437–1452.
5. Matkovic, M., Cavallini, A., del Col, D., Rossetto, L. (2009). Experimental study on condensation heat transfer inside a single circular minichannel. *International Journal Heat Mass Transfer*, 52, 2311–2323.
6. Fan, Y., Cui, X., Han, H., Lu, H., Wu, H. et al. (2019). Chiller fault diagnosis with the technology of imbalanced data. *Journal of Engineering Thermophysics*, 40(6), 1219–1228.
7. Liu, X., Zheng, Y., Wang, J., Lu, Z. (2019). Operational control strategy of non-uniform load matching for multiple chillers. *Journal of South China University of Technology (Natural Science Edition)*, 47(9), 24–32+39.
8. Tang, C., He, Y., Chen, Z. (2011). Numerical and experimental study on system performance of air-cooled scroll chiller. *Journal of Chongqing University*, 34(S1), 17–20+29.

9. Yu, P., Zhang, X. (2019). Performance of mixed refrigerant with different temperature glides in dual temperature water chillers. *Journal of Southeast University (Natural Science Edition)*, 49(5), 833–839.
10. Li, J. (2019). Discussion on oil return technology of water-cooled screw water chiller. *Refrigeration and Air-Conditioning*, 19(11), 38–41.
11. Kassim, G., Mahmood, M., Mahdi, L. (2022). Modeling of heat transfer and steam condensation inside a horizontal flattened tube. *Fluid Dynamics & Materials Processing*, 18(4), 985–998. <https://doi.org/10.32604/fdmp.2022.018938>
12. Mahmood, R. A., Buttsworth, D., Malpress, R. (2019). Computational and experimental investigation of the vertical flash tank separator. Part 1: Effect of parameters on separation efficiency. *International Journal of Air Conditioning and Refrigeration*, 27, 195–205.
13. Mahmood, R. A., Buttsworth, D., Malpress, R. (2019). Computational and experimental investigation of using an extractor in the vertical gravitational flash tank separator. *International Journal of Automotive and Mechanical Engineering*, 16, 6706–6722.
14. Mao, Q., Fang, X., Li, G., Liang, Z., Hu, Y. (2019). Chiller sensor fault detection using denoising-based improved principal component analysis. *Heating Ventilating & Air Conditioning*, 49(7), 106–110.
15. Li, D., Li, D., Zhang, S., Feng, S. (2018). Experimental research on application of R417A and R22 refrigerant mixture in low temperature air source heat pumps. *Fluid Machinery*, 46(9), 84–88+54.
16. Liu, Z., Zhang, Y., Li, X. (2019). Experimental study on characteristics of household CO₂ air-source heat pump water heater. *Fluid Machinery*, 47(2), 70–74.
17. Lu, X., Li, Q., Lu, F., Peng, C., Lin, C. et al. (2018). Experimental study on the effect of air flow and water consumption on the performance of air source heat pump hot water unit. *Fluid Machinery*, 46(12), 60–64.
18. Wu, X., Xu, S., Gui, X., He, Y., Guo, Q. (2019). Effect of water supply temperature on the performance of low temperature air source heat pump system. *Journal of Refrigeration*, 40(3), 66–71+78.
19. Yuan, Z., Tao, L., Yu, Z. (2017). Effect of initial water temperature on the performance of air-source heat pump water heater system. *Journal of Refrigeration*, 38(6), 73–79.
20. Shen, D., Gui, C., Xia, J., Xue, S. (2020). Experimental analysis of the performances of unit refrigeration systems based on parallel compressors with consideration of the volumetric and isentropic efficiency. *Fluid Dynamics & Materials Processing*, 16(3), 489–500. <https://doi.org/10.32604/fdmp.2020.08969>
21. Shen, D., Gui, C., Xia, J., Xue, S. (2020). A novel method for calculating correlation of flow condensation pressure drop in micro-fin tube. *UPB Scientific Bulletin, Series D: Mechanical Engineering*, 82(2), 143–160.
22. Oussama, R., Chaouki, G., Maamar, B. (2020). Modeling and simulation analysis of solar absorption chiller driven by nanofluid-based parabolic trough collectors (PTC) under hot climatic conditions. *Case Studies in Thermal Engineering*, 19, 145–158.
23. Kwon, O., Cha, D., Park, C. (2017). Performance evaluation of a two-stage compression heat pump system for district heating using waste energy. *Energy*, 57(8), 75–81. <https://doi.org/10.1016/j.energy.2013.05.012>
24. Kandlikar, S. G., Grande, W. J. (2003). Evolution of microchannel flow passages thermohydraulic performance and fabrication technology. *Heat Transfer Engineering*, 24(1), 3–17. <https://doi.org/10.1080/01457630304040>
25. Park, Y., Kim, Y., Cho, H. (2002). Thermodynamic analysis on the performance of a variable speed scroll compressor with refrigerant injection. *International Journal of Refrigeration*, 25(8), 1072–1082. [https://doi.org/10.1016/S0140-7007\(02\)00007-5](https://doi.org/10.1016/S0140-7007(02)00007-5)
26. Aprea, C., Mastrullo, R., Renno, C., Vanoli, G. (2004). An evaluation of R22 substitutes performances regulating continuously the compressor refrigeration capacity. *Applied Thermal Engineering*, 24(1), 127–139. [https://doi.org/10.1016/S1359-4311\(03\)00187-X](https://doi.org/10.1016/S1359-4311(03)00187-X)
27. Kasim, T., Ouedraogo, K. (2020). Effect of storage tanks on solar-powered absorption chiller cooling system performance. *International Journal of Energy Research*, 44(6), 4366–4375.
28. Li, G., He, Q., Du, D. (2019). A novel compressed air energy storage system with variable pressure ratio and its operation mode. *Automation of Electric Power Systems*, 43(8), 62–71.
29. Wu, K., Sun, S., Yang, L., Guo, P. (2018). Internal flow characteristics of scroll refrigeration compressor under different pressure ratio conditions. *Journal of Xi'an University of Technology*, 34(3), 338–343+370.